Proceedings of the 3rd International Conference on Mechanical Engineering and Mechatronics
Prague, Czech Republic, August 14-15, 2014
Paper No. 153

Dynamic Analysis of a Floating Cable-driven Platform for Marine Applications

Mamon Horoub, Mahir Hassan*, Muhammad Hawwa
King Fahd University of Petroleum and Minerals (KFUPM)
Department of Mechanical Engineering
Dhahran, 31261, Saudi Arabia
mahirhassan@kfupm.edu.sa

Abstract – This study investigates the dynamic behaviour of a floating cable-driven manipulator subjected to sea wave forces. The manipulator has six cables with a layout similar to that of Stewart Gough parallel manipulator. Positive tensions in the cables were maintained by applying varying cable pretension in the workspace to ensure non-negative cable forces. The displacement, velocity, and acceleration responses of the platform have been calculated in the entire workspace. At the boundaries of the workspace, greater pretensions and submerged depth are needed to operate the manipulator without loss of cable tensions.

***Keywords*:** Cable-driven manipulator, Workspace, Dynamics, Marine platform, Sea waves.

1. Introduction

Cable-driven parallel manipulators (CPM) are parallel manipulators that are based on cables instead of rigid-links. They are known for their large workspace and high acceleration capability, compared to those of rigid-link parallel manipulators. There have been a number of CPM designs presented in the literature such as NIST Robocrane (Albus et al., 1993), Falcon-7 (Kawamura et al., 1995), WARP (Maeda et al., 1999), WiRo (Ferraresi et al., 2004) DeltaBot (Behzadipour and Khajepour, 2005), and the hybrid cable-actuated robot developed by Mroz et al (2004). Because cables can only be under tension, many researchers have studied the ability of CPM's to achieve static equilibrium in the workspace with taut cables (Kawamura and Ito, 1993), (Diao and Ma, 2007). Other studies (Fang, 2004), (Hassan and Khajepour, 2008, 2011) focused on the optimization of cable forces in the manipulator. One potential application that has not been fully explored for cable-driven manipulators is in the marine environment. Tension leg platforms (TLPs) are examples of floating platforms fixed by cables anchored to the seabed. TLPs are offshore stations that are used to explore oil in deep water. This type of floating marine structures is nowadays used also in floating breakwater systems and the fish-farming cage systems (Lee and Wang, 1999, 2000, 2005). They constitute two parts: a semi-submerged structure and cables connected to the seabed. However, TLPs have certain limitations (Kareem, 1985), (Mostafa and El Naggar, 2004), one of which is the lack of their ability to change their horizontal position on the sea surface. Therefore, exploring the idea of using a cable-driven manipulator system to move these floating platforms along the sea surface can be of direct benefit to marine structures such as TLPs.

Other studies focused on the dynamical analysis in the tension leg platforms (TLPs). Lee and Wang (2001) presented a detailed analytical solution for the dynamic behavior of TLPs system. This study was for the case of the platform device is subjected to the wave-induced surge and drag motions. Chen et al. (2006) examined the coupled dynamic interaction between the hull of a floating platform and its risers and tendons. Bae and Kim (2013) investigated the coupled dynamics of a mono-column-TLP subjected to second-order sum–frequency wave excitations. This work analyzes the dynamics of a cable driven platform subjected to sea wave forces.

2. Sea Loads

The floating robotic platform is subjected to dynamic forces from the sea waves [24]. These waves may be caused by wind, tides, and earthquakes, and their shape is dependent on the forces acting on the water.

To determine the sea wave forces affecting the floating cable-driven platform, the platform will be considered as a circular disc, of radius “a” and draft “b” that can have surge, heave, and pitch motions. The water wave applied on the circular disc has amplitude of H/2 and angular frequency of ω as seen in Fig.1. The reference coordinate frame is located on still water level (SWL) and it is assumed that the wave moves along the x-axis.

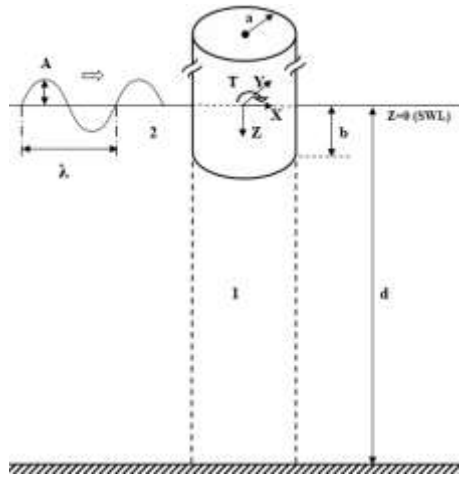

Fig. 1. Definition sketch for isolated cylinder.

Finnegan et al (2011) divided the fluid domain into two regions: an interior region under the cylinder (marked as 1 in Figure 1) and an exterior region (marked as 2 in Figure 1) that extends to infinity in the horizontal plane. The solution of the scattering and radiation problem for floating vertical cylinder (in infinite depth water) has been studied by Finnegan et al and they found an analytical solution for the water wave excitation forces on a floating cylinder as:

$$\hat{F}_x = -\frac{\pi i \rho g H a}{k_o}\left(J_1(k_o a) - \frac{J_1'(k_o a)}{\mathrm{H}_1'(k_o\, a)}\mathrm{H}_1(k_o a)\right)(1 - e^{-k_o b}) \quad (1)$$

$$\hat{F}_z = -2\pi i \rho \omega a \sqrt{\frac{2}{\pi}} \int_0^\infty P_0(\xi)\, \frac{I_1(\xi r)}{\xi I_0(\xi a)}\, d\xi \quad (2)$$

$$\hat{F}_T = T = -\pi i \rho g H a\left(J_1(k_o a) - \frac{J_1'(k_o a)}{\mathrm{H}_1'(k_o\, a)}\mathrm{H}_1(k_o a)\right)\int_0^b (z-b) e^{-k_o z}\, dz \quad (3)$$

$$+ \pi i \rho \omega a^2 \sqrt{\frac{2}{\pi}} \int_0^\infty P_1(\xi)\, \frac{I_2(\xi r)}{\xi I_1(\xi a)}\, d\xi$$

$$F_j = \hat{F}_j\, e^{-i\omega t}\ , \quad j = x, z \text{ and } T \quad (4)$$

where

- J_m denotes a Bessel function of the first kind of order m.
- I_m denotes a modified Bessel function of the first kind of order m.
- H_m is the Hankel function of the first kind of order m, primes denote differentiation with respect to argument.

- k_0 is the wavenumber.
- $H = 2A$.
- $P_m(\xi) = -\frac{gH}{2\omega}\epsilon_m i^{m+1}\sqrt{\frac{2}{\pi}}\left(J_m(k_o a) - \frac{J_m'(k_o a)}{H_m'(k_o\, a)} H_m(k_o a)\right)\frac{e^{-k_o b}k_o}{\xi^2 + {k_o}^2}$.
- ϵ_m is Neumann's number, ϵ_o= 1, ϵ_m= 2, m ≥ 1.

Figures 2-4 show the wave forces for assumed values of $b = 1.25\, m$; $a = 5\, m$; $d = 50\, m$; $k_o = 0.16095\, m^{-1}$; $H = 0.2\, m$; $g = 9.81\, \frac{m^2}{s}$, $\rho = 1000\, \frac{kg}{m^3}$.

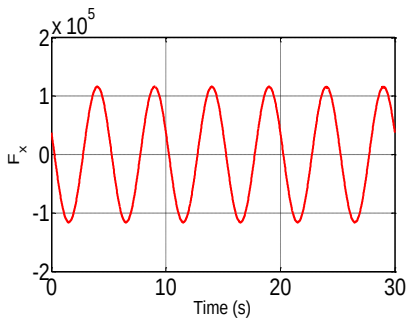

Fig.2. Surge excitation force.

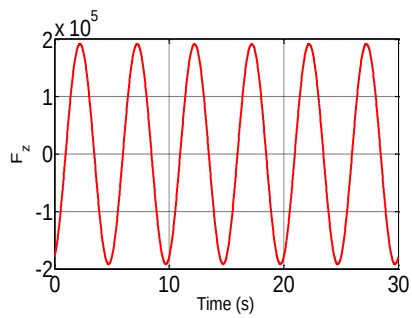

Fig.3. Heave excitation force.

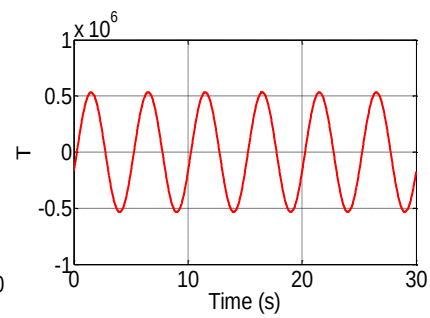

Fig.4. Pitch excitation force.

The sea also exerts a static upward force (buoyant force F_B) which equals in magnitude to the weight of the fluid displaced by the object. This force is applied as vertical force on the floating platform and can be calculated as:

$$F_b = \rho V g \tag{5}$$

Where ρ is the object density, g is the gravity acceleration, and $V = d\pi a^2$ is the submerged volume of the floating platform.

3. Layout of the Floating Cable-driven Platform

The layout of the floating cable-driven platform is shown in Figs. 5 and 6. It consists of six cables driven by motors/reels mounted on the surface of the floating platform and anchored in the seabed. It consists of six cables arranged in a form similar to the Stewart Gough parallel robot, depicted in Fig.6. The anchored ends of the six cables (i=1,…, 6) are located at angles $90, 120, 210, 240, 330$ degrees, respectively, around the perimeter of the base circle on the sea bed. Also, these six cables are driven by six motors on the surface of the platform (circular disc with radius 5 m) located at points $B_1, B_2, B_3, B_4, B_5, B_6$ at angles $30, 120, 150, 240, 270$ respectively. The distance between the base and the platform is 0.5 m, which is the assumed water depth.

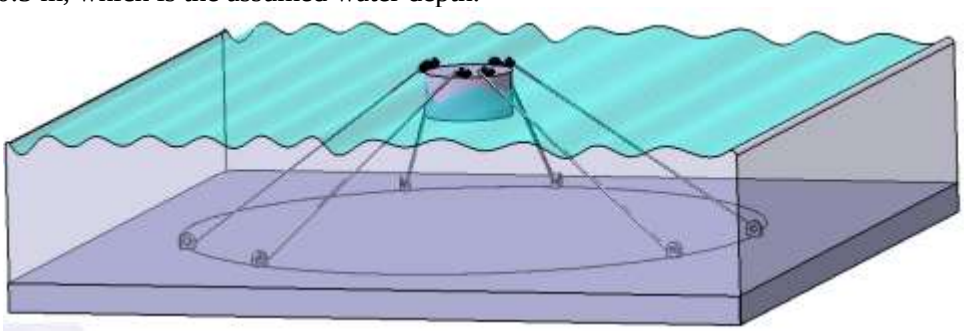

Fig.5. Floating cable-driven platform.

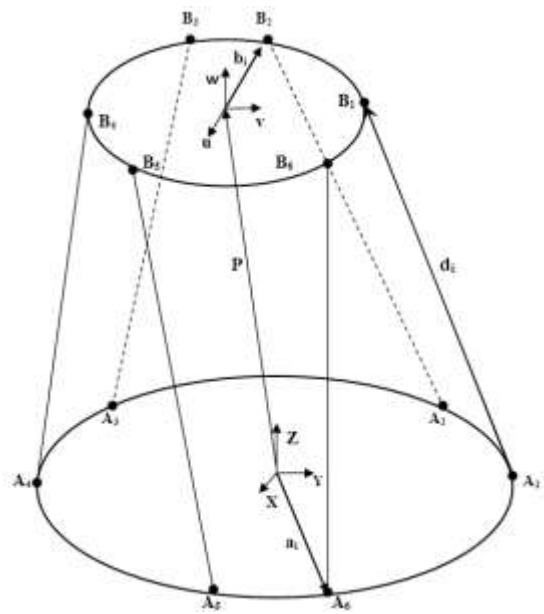

Fig.6. The schematic drawing of the 6-DOF parallel manipulator.

4. Dynamic Model

Equation (6) represents the dynamics of the moving platform. K is the stiffness, M is the mass matrix and F is the sea wave forces.

$$M\ddot{x} + Kx = F \tag{6}$$

where

$$x = [\, p_x \quad p_y \quad p_z \quad \theta_x \quad \theta_y \quad \theta_z \,]^T$$
$$F = [\, F_x \quad 0 \quad F_z \quad 0 \quad T \quad 0 \,]^T$$

Solving Equation (6) using the modal analysis method the uncoupled differential equations of 6 orders as follows:

$$\ddot{q}_i(t) + \omega_i^2 q_i(t) = Q_i(t) \tag{7}$$
$$Q_i(t) = U^T F \tag{8}$$

where ω_i is the ith natural frequencies of the system, U is the modal matrix, $i = 1, 2, 3 \ldots .6$.
Equation (7) can be solved as:

$$q_i(t) = \frac{1}{\omega_i} \int_0^t Q_i(\tau) \sin \omega_i (t - \tau)\, d\tau \,, i = 1,2, \ldots .6 \tag{9}$$

Equation (9) can be represented using the original states vector (x vector) as follows:

$$x_i(t) = U q_i(t) \tag{10}$$

which can be differentiated to determine the velocity and the acceleration of the platform.

The cable tensions, platform position, velocity and acceleration of the platform with time at the center pose are shown in Figures 7, 8, 9, and 10.

The workspace of the manipulator is characterized here as the set of platform poses (position and orientation) in which platform can balance the external forces, i.e., weight, buoyancy, and wave loads, with positive cable tensions.

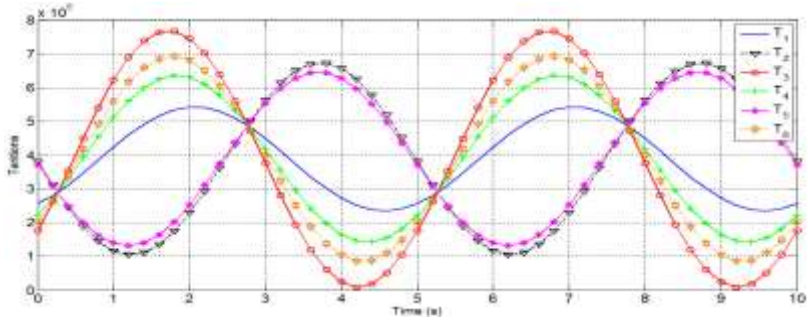

Fig. 7. The six cable tensions at center pose.

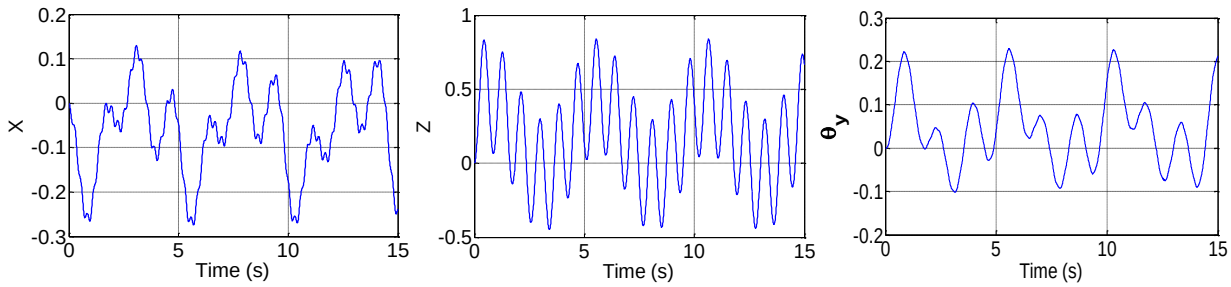

Fig. 8. The platform x, z, and theta-y displacements at center pose of workspace.

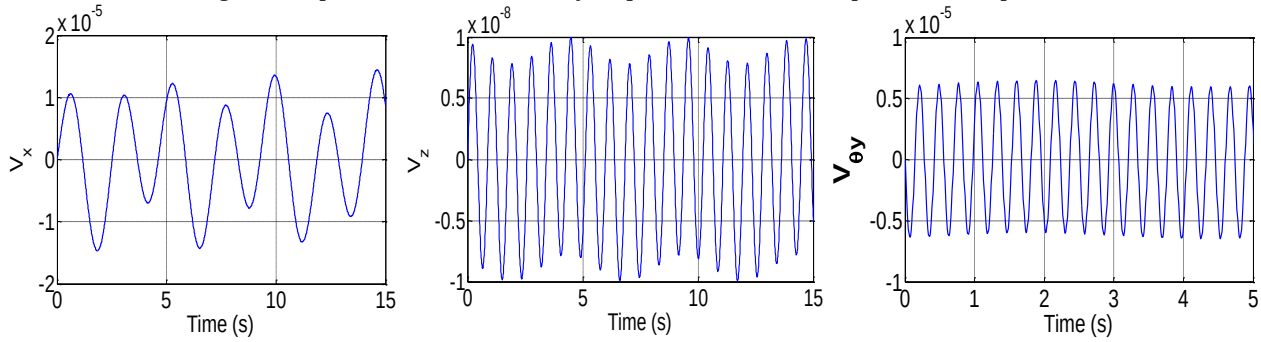

Fig. 9. The platform velocity in the x, z, and theta-y coordinates at center pose of workspace.

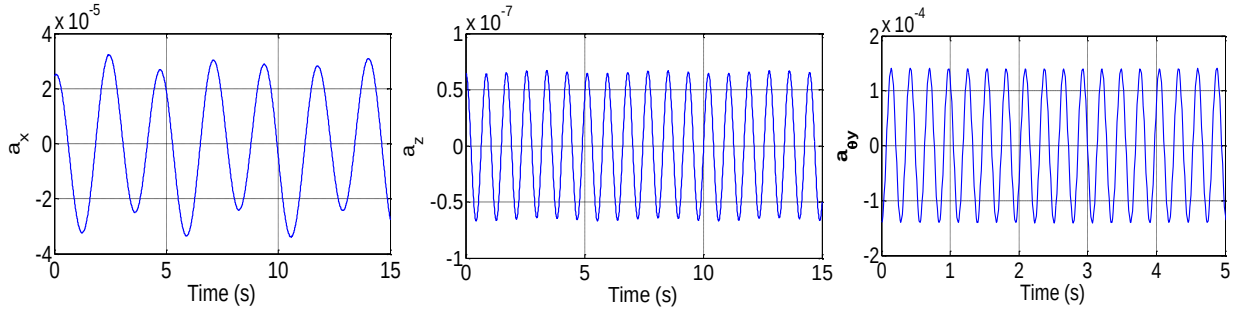

Fig. 10. The platform acceleration in the x, z, and theta-y coordinates at center pose of workspace.

4. Global Dynamic Analysis

The dynamic analysis in the previous section was at the center pose only. In this section the analysis is repeated at discrete points in the workspace and the norm value of the Root Mean Square (RMS) of the cable tension, displacement, velocity, and acceleration are plotted across the workspace in order to have any idea about the variation of the dynamic performance of the platform in the workspace.

At each pose, positive tensions in the cables are maintained by applying pretension, resulting in increasing the submerged depth (b) of the platform. When the platform moves from one pose to another in the workspace, the magnitude of the pretension applied in the cables is the minimum required to ensure that cable tensions are non-negative. Applying pretension changes the vertical submerged depth of the platform as shown in Fig. 11. As a result, the forces in Equations 1-5 are recalculated in at each pose based on the minimum submerged depth needed at those poses to ensure non-negative cable tensions. Figure 11 indicates that the submerged depth needed near the boundary of the workspace is greater than that needed near the center to ensure non-negative cable tensions and, hence, resulting in higher tensions (as shown in Fig. 12) required to operate the manipulator at the workspace boundaries.

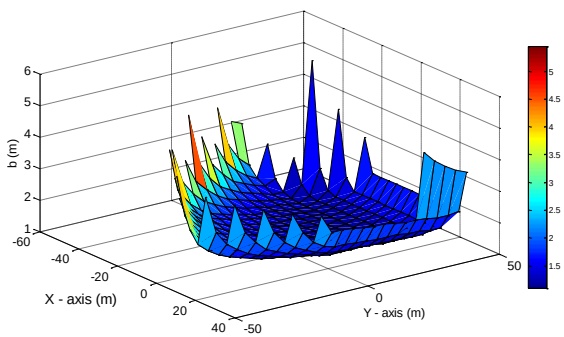

Fig. 11. Minimum submerged depth required at each pose in the workspace, to maintain positive tensions.

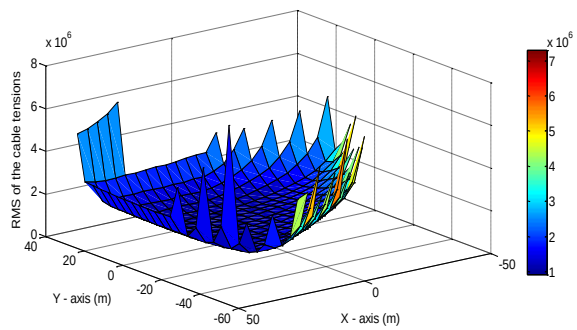

Fig. 12. The 2-norm value of the six RMS values of the cable tensions at each pose in the workspace, for the specified submerged depth.

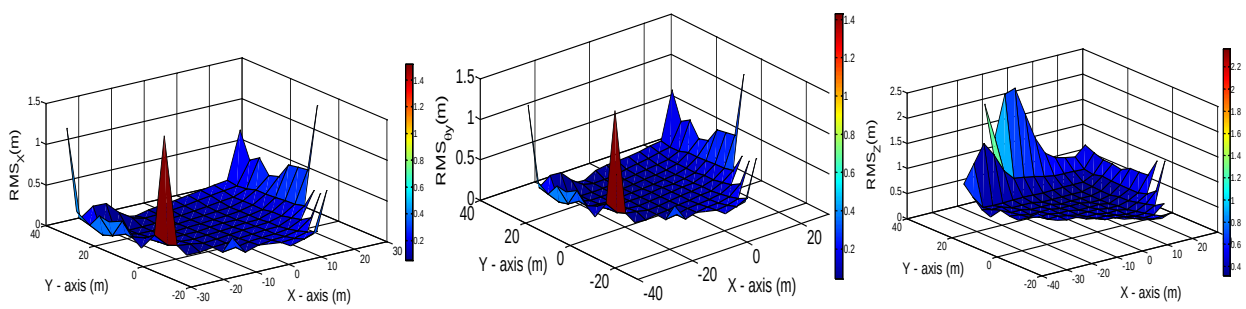

Fig. 13. RMS values of the x, z, and theta-y displacement components at each pose in the workspace.

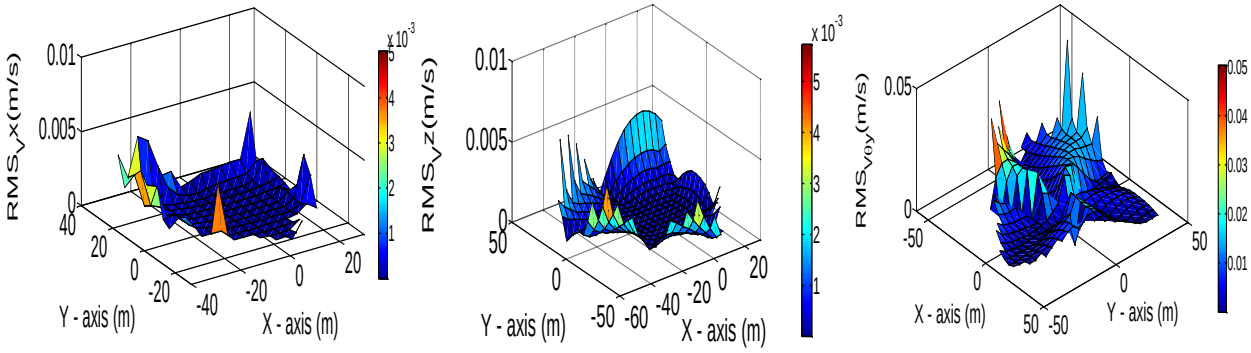

Fig. 14. RMS values of the x, z, and theta-y velocity components at each pose in the workspace.

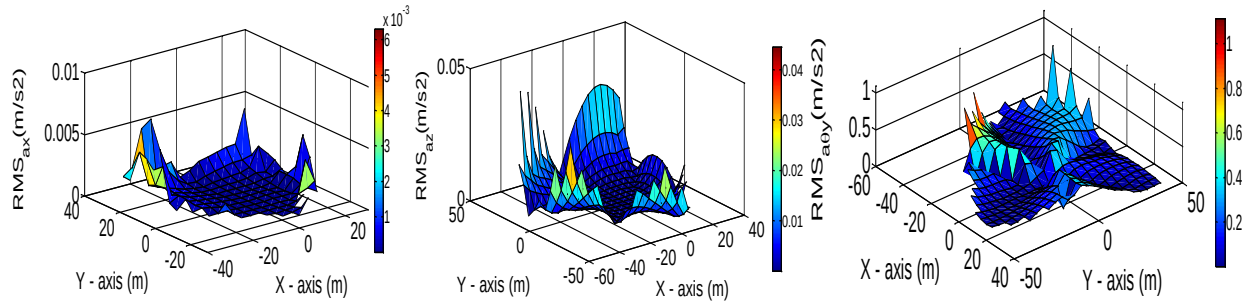

Fig. 15. RMS values of the x, z, and theta-y acceleration components at each pose in the workspace.

5. Conclusion

The dynamic behaviour of a floating cable-driven manipulator subjected to sea waves was analyzed in this study. The platform positive tensions were maintained by applying cable pretension and, hence, varying the submerged depth of the platform. The displacement, velocity, and acceleration responses of the platform have been calculated in the entire workspace. It is shown that greater tensions and submerged depth are needed to operate the manipulator at the boundaries of the workspace. This study focused on cable layout similar to the famous Stewart Gough parallel manipulator.

Acknowledgements

The author(s) would like to acknowledge the support provided by King Abdulaziz City for Science and Technology (KACST) through the Science & Technology Unit at King Fahd University of Petroleum & Minerals (KFUPM) for funding this work through project No. 11-ELE1623-04 as part of the National Science, Technology and Innovation Plan.

References

Albus J., Bostelman R., Dagalakis N. (1993). The Nist Robocrane, J. Robotic Systems, vol. 10, n. 5,709-724.

Bae Y.H., Kim M.H. (2013) " Rotor-floater-tether coupled dynamics including second-order sum–frequency wave loads for a mono-column-TLP-type FOWT (floating offshore wind turbine)", Ocean Engineering 61,109–122.

Behzadipour S., Khajepour A. (2005). A New Cable-based Parallel Robot with Three Degrees of Freedom, *Multibody System Dynamics*, vol. 13, pp. 371-383.

Chen X., Ding Y., Zhanga J., Liagre P., Niedzwecki J., Teigen P. (2006) Coupled dynamic analysis of a mini TLP: Comparison with measurements', Ocean Engineering 33, 93–117.

Diao X., Ma O. (2007), “Force-closure Analysis of General 6-DOF Cable Manipulators” in *Proc. IEEE/RSJ Int. Conf. Intell. Robots and Systems*, San Diego, USA, pp. 3931-3936.

Fang S., Franitza D., Torlo M., Bekes F., Hiller M. (2004). “Motion Control of a Tendon-Based Parallel Manipulator Using Optimal Tension Distribution”, *IEEE/ASME Trans. Mechatronics*, vol. 9, no. 3, pp. 561-568.

Kawamura S., Choe W., Tanak S. (1995), Development of an Ultrahigh Speed Robot Falcon Using Wire Driven Systems, *Proc. IEEE Int. Conf. on Robot. Autom.*, 215-220.

Maeda K., Tadokoro S., Takamori T., Hiller M., Verhoeven R (1999). On Design of a Redundant Wire-driven Parallel Robot WARP Manipulator in *Proc. IEEE Int. Conf. on Robot. Autom.*, vol. 2, pp. 895-900.

Ferraresi C, Paoloni M., Pescarmona F. (2004). A new 6-dof Parallel Robotic Structure Actuated by Wires: The Wiro-6.3, *J. of Robotic Systems*, vol. 21, no. 11, pp. 581-595.

Finnegan W., Meere M., Goggins J. (2011). The Wave Excitation Forces on a Floating Vertical Cylinder in Water of Infinite Depth. World Renewable Energy Congress.

Hassan M., Khajepour A. (2008). “Minimum-norm Solutions for the Actuator Forces in Cable-based Parallel Manipulators Using Convex Analysis and Optimization”, *IEEE Transactions on Robotics*, vo. 24 (3), pp. 736-740.

Hassan M., Khajepour A. (2011). “Analysis of Bounded Cable Tensions in Cable-actuated Manipulators”, *IEEE Transactions on Robotics*, vol. 27, no. 5, pp. 891-900.

Kareem A., (1985) Wind Induced Response Analysis of Tension Leg Platforms.” J. Struct. Eng., 111(1), pp. 37–55.

Kawamura S., Ito K (1993). A New Type of Master Robot for Teleoperation Using a Radial Wire Drive System, in *Proc. IEEE Int. Conf. Intell. Robots and Systems*, pp. 55-60.

Lee H. H., and Wang P.-W, Lee C.-P. (1999). Dragged surge motion of tension leg platforms and strained elastic tethers", Ocean Engineering 26, pp.575–594.

Lee H. H., and Wang P.-W. (2000) Analytical solution on the surge motion of tension-leg twin platform structural systems, Volume 27, Issue 4, pp. 393–415.

Lee H. H., Wang W. S. (2001), "Analytical solution on the dragged surge vibration of tension leg platforms (TLPs) with wave large body and small body multi-interactions", Journal of Sound and vibration, 248(3), 533-556.

Lee H. H., Wang W.-S. (2005). The Dragged Surge Motion Of Tension-Leg Type Fish Cage System Subjected To Multi-Interactions Among Wave And Structures", IEEE Journal Of Oceanic

Mostafa Y. E., El Naggar M. H. (2004). 'Response of fixed offshore platforms to wave and current loading

Mroz G, Notash., L. (2004) Wire-actuated Robots with a Constraining Linkage, *J. Robotic Systems*, vol. 21, no. 12, pp. 677-678.